Global simulation of tropospheric O 3 -NO x -hydrocarbon chemistry: 3. Origin of tropospheric ozone and effects of nonmethane hydrocarbons

Share Your Story

The Harvard community has made this article openly available.
Please share how this access benefits you. Submit a story .

Accessibility

Global simulation of tropospheric O_3-NO_x-hydrocarbon chemistry

3. Origin of tropospheric ozone and effects of nonmethane hydrocarbons

Yuhang Wang,[1] Daniel J. Jacob, and Jennifer A. Logan

Department of Earth and Planetary Sciences and Division of Engineering and Applied Sciences, Harvard University, Cambridge, MA 02138

Abstract. A global three-dimensional model of tropospheric O_3-NO_x-hydrocarbon chemistry is used to investigate the factors controlling ozone concentrations in the troposphere. Model results indicate a close balance between chemical production and chemical loss of ozone in the tropospheric column at all latitudes (except high latitudes in winter). Using separate tracers for ozone produced in the stratosphere and in different regions of the troposphere, we find that the contribution of transport from the stratosphere to ozone concentrations in the troposphere is about 30% at midlatitudes in winter, 10% in summer, and 5% in the tropics. Production of ozone in the upper, middle, and continental lower troposphere all make significant contributions (10-50%) to ozone concentrations throughout the troposphere. The middle troposphere is a major global source region for ozone even though it is not a region of net production. The springtime maximum of ozone observed at remote sites in the northern extratropics is explained by a phase overlap between ozone transported from the stratosphere which peaks in late winter and ozone produced in the troposphere which peaks in late spring. Our model results do not support previous explanations of the springtime maximum based on wintertime accumulation of ozone or its precursors in the Arctic. The particularly strong springtime maximum at Mauna Loa Observatory (Hawaii) is attributed to long-range transport of Asian pollution over the North Pacific in spring. A sensitivity simulation without nonmethane hydrocarbons (NMHCs) indicates small decreases of ozone concentrations (<15%) in the remote troposphere and a 20% increase in the global mean OH concentration. Without NMHCs as a source of peroxyacetylnitrate, concentrations of NO_x decrease by 30% in the remote lower troposphere but increase by 70% in the continental lower troposphere and by 40% in the upper troposphere. Biogenic isoprene accounts for about half of the NMHC effects in the model.

1. Introduction

This paper is the third of a series applying a global three-dimensional model to simulate tropospheric O_3-NO_x-hydrocarbon chemistry and to analyze the factors controlling tropospheric ozone. The model is described by *Wang et al.* [this issue(a)] and is evaluated with observations by *Wang et al.* [this issue(b)]. Here we use the model to investigate the origin of tropospheric ozone and to assess the role of nonmethane hydrocarbons (NMHCs) in modifying ozone, OH, and NO_x (NO+NO_2) concentrations in the troposphere.

We begin by examining the relative importance of different source regions for tropospheric ozone. Transport from the stratosphere was long thought to be the dominant source of ozone in the troposphere [*Junge*, 1962; *Danielsen*, 1964]. In the early 1970s, *Crutzen* [1973] and *Chameides and Walker* [1973] suggested instead that tropospheric ozone originates mainly from production within the troposphere by photochemical oxidation of CO and hydrocarbons catalyzed by NO_x and HO_x (OH + HO_2). By the mid 1980s, global budget analyses

indicated that chemical production of ozone within the troposphere was at least as large as transport from the stratosphere, although with large uncertainties due in part to limited observations of NO_x concentrations [e.g., *Fishman*, 1985]. *Liu et al.* [1987] calculated the in situ production of tropospheric ozone in the northern hemisphere by scaling hemispheric estimates of NO_x emissions with the ozone production efficiency (ozone molecules produced per NO_x molecule oxidized); they concluded that this in situ source of ozone was much larger than transport from the stratosphere.

The emergence over the past decade of a large database of aircraft observations for NO concentrations in the remote troposphere has improved significantly the constraints for calculating regional and global ozone budgets [*Carroll and Thompson*, 1995; *Bradshaw et al.*, 1998]. These data indicate that ozone in the remote troposphere is often in close balance between chemical production and chemical loss [*Chameides et al.*, 1987, 1989; *Liu et al.*, 1992]. A recent photochemical model analysis of aircraft observations in the tropical troposphere suggests that ozone concentrations are controlled by chemical steady state over the scale of the tropospheric column [*Jacob et al.*, 1996].

Analyses of atmospheric observations and the current generation of global three-dimensional models of tropospheric chemistry [*Crutzen*, 1994; *Müller and Brasseur*, 1995; *Roelofs and Lelieveld*, 1995; *Wang et al.*, this issue(b)] all support the view that the global budget of tropospheric ozone is largely controlled by photochemical production and loss within the troposphere. Much less work has been conducted to investigate the relative contributions of different tropospheric source regions to ozone levels. Such regional source attribution is complicated by the nonlinearity of ozone chemistry and by the variability in the lifetime of ozone, which may range from less than a week to several months for different regions of the troposphere. In the present paper, we approach this issue by tracing separately in our global three-dimensional model ozone molecules produced in different regions of the troposphere and in the stratosphere. We can in this manner quantify the contributions to tropospheric ozone concentrations from production in the stratosphere [*Levy et al.*, 1985], the upper troposphere [*Liu et al.*, 1980; *Liu*, 1988; *Jacob et al.*, 1996], the polluted continental boundary layer [*Jacob et al.*, 1993; *Liang et al.*, 1998], as well as the middle troposphere and the marine boundary layer.

One specific application of our ozone source region analysis is to understand the origin of the springtime ozone maximum observed in the lower troposphere at remote northern extratropical sites [*Logan*, 1985]. A number of hypotheses have been proposed to explain this feature. *Logan* [1985] suggested that the springtime maximum is caused by cross-tropopause transport of stratospheric ozone, in contrast to the summertime maximum at polluted U.S. and European sites which is associated with photochemical production. In a global three-dimensional simulation of tropospheric ozone with a source from the stratosphere and deposition at the surface but no chemistry, *Levy et al.* [1985] found that surface ozone in the northern hemisphere exhibits a ubiquitous springtime maximum supporting the view that this maximum is due to the

cross-tropopause transport of stratospheric ozone. On the other hand, *Penkett and Brice* [1986] found that peroxyacetylnitrate (PAN) concentrations in background air over Europe have a springtime maximum, suggesting that the intensifying photochemistry in spring may be responsible for the observed ozone maximum. *Liu et al.* [1987] proposed that wintertime accumulation of ozone produced from anthropogenic NO_x could contribute to the springtime maximum. Wintertime accumulation of ozone precursors (total reactive nitrogen NO_y and hydrocarbons) in the Arctic has also been proposed as a possible source for enhanced ozone production in spring as the precursors become photochemically active [*Honrath and Jaffe*, 1992; *Honrath et al.*, 1996]. Our model reproduces the observed springtime maximum in ozone at remote sites in the northern extratropics [*Wang et al.*, this issue(b)], thus providing a useful tool for investigating this feature.

We will also explore in the model the extent to which emissions of NMHCs affect tropospheric ozone, OH, and NO_x concentrations. Previous three-dimensional global models for tropospheric ozone have often ignored NMHC chemistry [*Crutzen and Zimmermann*, 1991; *Roelofs and Lelieveld*, 1995, 1997]. However, NMHCs have some important effects on tropospheric chemistry. They increase the ozone production efficiency per unit NO_x in the continental boundary layer [*Lin et al.*, 1988]. They form organic nitrates such as PAN which provide reservoirs for the long-range transport of anthropogenic NO_x to the remote atmosphere [*Singh and Hanst*, 1981; *Jacob et al.*, 1992; *Fan et al.*, 1994; *Moxim et al.*, 1996]. They provide a sink for OH [*Kasting and Singh*, 1986] but also provide a source of HO_x due to photolysis of NMHC oxidation products such as formaldehyde and acetone [*Sillman et al.*, 1990; *Singh et al.*, 1995]. A global three-dimensional model is necessary to investigate how these combined effects of NMHCs on tropospheric chemistry may affect ozone concentrations.

We describe briefly in section 2 the formulation and evaluation of the model; further details are in the companion papers [*Wang et al.*, this issue (a,b)]. Section 3 presents our analysis of the relative contributions of different source regions to tropospheric ozone concentrations. The origin of the springtime ozone maximum in the remote lower troposphere of the northern extratropics is discussed in section 4. The effects of NMHCs are discussed in section 5, followed by conclusions in section 6.

2. Model

The model is driven by meteorological fields with 4-hour temporal resolution from a general circulation model (GCM) developed at the Goddard Institute for Space Studies [*Hansen et al.*, 1983]. It has a spatial resolution of 4° latitude by 5° longitude with seven vertical layers extending from the surface to 150 mbar. Fifteen chemical tracers are transported: odd oxygen ($O_x = O_3 + O + NO_2 + HNO_4 + 2 \times NO_3 + 3 \times N_2O_5$), NO_x ($NO + NO_2 + NO_3 + HNO_2$), N_2O_5, HNO_3, HNO_4, peroxyacylnitrates, alkylnitrates, CO, ethane, ($\geq C_4$) alkanes, ($\geq C_3$) alkenes, isoprene, acetone, ($\geq C_4$) ketones, and H_2O_2. The

model solves the continuity equation for each tracer including terms for chemistry, emission, transport, and deposition. Transport across the tropopause in the model is specified as a flux boundary condition at 150 mbar varying monthly and spatially. The global mean cross-tropopause flux of ozone (401 Tg O_3 yr^{-1}) is distributed mainly between 20° and 60° latitude in both hemispheres. It has a broad January-May maximum in the northern hemisphere and a sharper July maximum in the southern hemisphere. Although the model tropopause is considerably higher than observed in the winter extratropics (300-400 mbar) the implications for our analysis are small because the 150- to 400- mbar column is chemically inert in winter.

Figure 1 shows the simulated zonal mean concentrations of ozone, OH, NO_x, and PAN for January and July. *Wang et al.* [this issue(b)] presented an extensive evaluation of model results using long-term surface observations of ozone, CO, and C_2H_6; climatological ozonesonde data; and aircraft measurements of NO, PAN, HNO_3, C_2H_6, acetone, and H_2O_2 in various regions of the troposphere. The model simulates ozone concentrations usually to within 10 parts per billion by volume (ppbv) and captures the observed seasonality of ozone in different regions of the troposphere to within 1 month. The principal model flaws identified for ozone are an underestimate in the upper troposphere of the southern tropics and an overestimate in the tropical marine lower troposphere. Simulated NO and PAN concentrations in different regions of the troposphere are usually in agreement with observations to within a factor of 2. HNO_3 is generally overestimated by the model, which we interpret as reflecting unaccounted sinks that do not lead to rapid recycling of NO_x; this overestimate is of little consequence for the results discussed below owing to the low reactivity of HNO_3 and its efficient removal by deposition. The model lifetime of CH_3CCl_3 against oxidation by OH is 5.1 years below 200 mbar, in close agreement with the estimate of 4.9 ± 0.3 years derived by *Prinn et al.* [1995] from long-term observations of CH_3CCl_3.

3. Source Regions for Tropospheric Ozone

Ozone in the troposphere cycles chemically with other species of the odd oxygen family ($O_x = O_3 + O + NO_2 + HNO_4 + 2$ x $NO_3 + 3$ x $N_2O_5 + PANs + HNO_3$). The budget of ozone is most appropriately expressed on the basis of production and loss rates of O_x. Since ozone accounts for over 95% of O_x, we can regard the budgets of ozone and O_x as equivalent, and we will hereinafter refer to ozone instead of O_x for clarity. The main source of O_x in the troposphere (gross production) is the reaction of peroxy radicals with NO, and the main sinks are the reactions $O^1D + H_2O$, $O_3 + HO_2$, and $O_3 + OH$. The resulting global budget for tropospheric ozone in our model [*Wang et al.*, this issue(b)] is dominated by in situ chemical production and loss (4100 and 3700 Tg O_3 yr^{-1}, respectively). Transport from the stratosphere (400 Tg yr^{-1}) is 10 times smaller than in situ chemical production; loss by dry deposition (800 Tg yr^{-1}) is also much smaller than in situ chemical loss. Our

Figure 1

result that the budget of tropospheric ozone is controlled on a global scale by in situ production and loss is in agreement with other global three-dimensional models [*Crutzen*, 1994; *Müller and Brasseur*, 1995; *Roelofs and Lelieveld*, 1995].

Figure 2 shows the latitudinal distributions of sources and sinks of ozone in the tropospheric column: chemical production and loss, transport from the stratosphere, and dry deposition. Production and loss are in approximate balance at all latitudes and are much larger than the stratospheric source except at high latitudes in winter. Ozone production is largest in the tropical troposphere (on an annual basis), and a close balance is found there between chemical production and loss, supporting the view that the tropical troposphere is self-sustaining with respect to ozone [*Jacob et al.*, 1996]. The surplus production at northern midlatitudes reflects large emissions of NO_x from fossil fuel combustion and is balanced in part by deposition to land surfaces.

We used the model to investigate the contributions to tropospheric ozone concentrations from five different source regions: the stratosphere, the upper troposphere (150 to 400 mbar), the middle troposphere (400 to 700 mbar), and the continental and marine lower troposphere (below 700 mbar). For this purpose, we transported in the model five separate O_x tracers originating from production in each of the above regions. These tracers were removed by chemical loss and dry deposition at the same frequencies as those for total O_x in the standard simulation. The sum of concentrations of all five O_x tracers is thus equal to the O_x concentration in the standard simulation, and the relative fraction from each tracer represents the contribution of the corresponding source region to ozone concentrations.

Figure 3 shows the fractional contributions from each source region to zonally averaged ozone concentrations as a function of pressure and latitude for January and July. Ozone produced in the stratosphere accounts for 20 to 40% of tropospheric ozone in the extratropical winter hemisphere, 5 to 20% in the summer hemisphere, and 5% in the tropics. Our results suggest a greater stratospheric influence on ozone concentrations near the surface than that obtained by *Follows and Austin* [1992] (<5% in all seasons) in a two-dimensional model study but a smaller influence than that obtained by *Roelofs and Lelieveld* [1997] in a three-dimensional simulation (10% in summer and 60% in winter). The discrepancy with *Roelofs and Lelieveld* [1997] reflects in part differences in the accounting of the stratospheric source. *Roelofs and Lelieveld* [1997] included as part of the stratospheric source any ozone molecule produced in the troposphere but having transited above the tropopause at some point in its history; the stratospheric source defined in this manner is twice as large in their model as the actual net downward transport of ozone across the tropopause. In comparison with our model, *Roelofs and Lelieveld* [1997] also have a 15% larger global cross-tropopause flux and 20% less tropospheric production, both of which contribute to a stronger stratospheric influence.

We find in our model that transport from the stratosphere contributes 15% to the global inventory of tropospheric ozone (20-25% in the winter hemisphere and 10% in the summer hemisphere), although it contributes only 9% to the global

Figure 2

Figure 3

source. The reason for this difference is that cross-tropopause transport takes place in the extratropical upper troposphere, where the lifetime of ozone is considerably longer than it is in the lower troposphere or in the tropics. We investigated this effect further by conducting a simulation without a stratospheric source of ozone (zero-flux boundary condition for ozone at 150 mbar; the model was initialized with observed ozone concentrations to provide an initial source of HO_x radicals). We found that ozone concentrations decreased from the standard simulation in proportions similar to those shown in Figure 3, indicating little nonlinearity in the response of ozone concentrations to suppression of the stratospheric source.

Model results in Figure 3 show that sources of ozone in the upper, middle, and continental lower troposphere all make significant contributions (10-50%) to ozone concentrations at all altitudes in the troposphere. There are, however, large differences with altitude and season in the rates of ozone production and loss. Figure 4 shows the distributions of zonally averaged gross production rate, net production rate (gross production minus loss), and lifetime against chemical loss of ozone in the model for January and July. Ozone production is much faster in the continental lower troposphere than in the upper troposphere, but the contributions from these two regions to ozone inventories are similar in much of the troposphere because the lifetime of ozone in the upper troposphere is much longer (2-6 months), allowing the accumulation of ozone from a relatively small production rate. In contrast, the short lifetime of ozone in the lower troposphere in summer (1-3 weeks) limits the range of influence of this large ozone source. Although chemical production and loss of ozone are roughly in balance in the middle troposphere, the large gross production rate (1-5 ppbv day^{-1}) coupled with a relatively long lifetime (1-3 months) results in a 20-40% influence of the middle tropospheric source on ozone concentrations throughout most of the troposphere. This influence is as large as that of the polluted lower troposphere or the upper troposphere, where net production of ozone takes place.

A few studies have attempted previously to determine source regions for tropospheric ozone by examining correlations with radiogenic tracers (^{7}Be and ^{210}Pb). Beryllium 7 is produced by cosmic rays in the stratosphere and the upper troposphere, while ^{210}Pb is a decay product of ^{222}Rn emitted from soils. *Dibb et al.* [1992] suggested that stratospheric input makes an important contribution to the ozone budget in the summer sub-Arctic troposphere, based on aircraft observations of elevated ^{7}Be and ^{210}Pb concentrations at about 4-km altitude which they ascribed to stratospheric influence. This result differs from our model where only about 10% of ozone at 0-6 km in the summer sub-Arctic is from the stratosphere. On the other hand, *Dibb et al.* [1994] used surface observations of ^{7}Be and ^{10}Be at Alert, Canada, to suggest that the stratospheric contribution to surface ozone at that site is only 10-15% in spring and less in other seasons; our model indicates a similarly low stratospheric contribution (5-15%). *Dibb et al.* [1996] found that over the western North Pacific in the fall, ozone was strongly correlated with ^{210}Pb originating from the Asian continent but not with ^{7}Be (the range of ^{7}Be concen-

Figure 4

trations there was however similar to the observations in the sub-Arctic). They inferred a large influence of Asian outflow on tropospheric ozone concentrations over the western Pacific and our model results lead to the same conclusion. Another study by *Prospero et al.* [1995] found that summertime ozone concentrations at Tenerife in the Canary Islands (altitude of 2.4 km) are correlated with [7]Be but anticorrelated with anthropogenic aerosols. They suggested that high-ozone air is associated with either ozone production in the free troposphere or transport from the stratosphere. Our model results indicate that 60% of ozone at Tenerife in summer originates from production in the upper and middle troposphere, while 7% is from the stratosphere.

4. Springtime Ozone Maximum in the Northern Extratropics

We show in a companion paper [*Wang et al.*, this issue(b)] that our model reproduces well the springtime ozone maximum observed in the lower troposphere at remote sites of the northern extratropics [*Logan*, 1985]. We examine here the origin of this maximum by decomposing the seasonal variation of ozone in the model into the contributions from different source regions. Figure 5 shows the results for a typical midlatitude site (Goose Bay, Canada). The April maximum at this site reflects the superimposed contributions of ozone transported from the stratosphere which peaks in January-April and ozone produced within the troposphere which peaks in April-June. Both chemistry within the troposphere and transport from the stratosphere contribute to shaping the springtime maximum, although chemistry is more important.

Also shown in Figure 5 is the seasonal variation of ozone concentrations at Mauna Loa Observatory, Hawaii. This tropical site (20°N) displays a particularly pronounced spring maximum, which has been ascribed to the same phenomenon as at northern midlatitudes [*Levy et al.*, 1985; *Logan*, 1985; *Ridley et al.*, 1997]. This pronounced spring maximum is reproduced by the model (Figure 5), where it reflects mostly the seasonal transport of ozone pollution from the Asian continent. Analyses of aerosol observations at island sites in the North Pacific have previously shown that the continental influence from Asia peaks in spring [*Merrill*, 1989], a result well captured in our model [*Balkanski et al.*, 1992].

In contrast to the spring maximum of ozone at remote sites, polluted sites in the northern extratropics have a broad summer maximum [*Logan*, 1985, 1989]. We find in the model that this contrast reflects not only a greater stratospheric influence at remote sites, but more importantly an earlier seasonal peak for ozone produced chemically within the troposphere. Figure 6 shows the seasonal variation of zonal mean ozone concentrations simulated by the model at 30°-90°N in the lower troposphere (below 700 mbar). Remote and polluted regions are separated on the basis of NO_x emissions from fossil fuel combustion; grid squares with emissions of less than 2×10^{11} molecules cm^{-2} s^{-1} are labeled as remote, while others are labeled as polluted. The summer maximum of ozone in polluted regions is controlled principally by production within the continental lower troposphere, which is largest in summer because

Figure 5

Figure 6

of high UV radiation and temperature [*Hirsch et al.*, 1996]. In remote regions, by contrast, ozone of tropospheric origin is mostly transported from long distances because local ozone production is weak. This transport is more efficient in spring than in summer because of the longer lifetime of ozone in spring, resulting in the earlier April-June maximum for ozone of tropospheric origin at remote sites.

Our model results do not support previous hypotheses that the springtime ozone maximum is due to wintertime accumulation at high latitudes of ozone precursors (PAN and NMHCs) [*Honrath et al.*, 1996] or ozone itself [*Liu et al.*, 1987]. Excluding the emissions of NMHCs and acetone from the model, and hence suppressing any accumulation of PAN or NMHCs, does not alter significantly the simulated ozone seasonality. We also find in the model no significant accumulation of ozone at northern high latitudes from December to February. Ozone production in winter may have been overestimated by *Liu et al.* [1987] because they did not account for the loss of NO_x by N_2O_5 hydrolysis on aerosol surfaces, which is the principal sink for NO_x in winter [*Dentener and Crutzen*, 1993].

5. Effects of NMHCs on Tropospheric Chemistry

We explored the role of NMHCs in modifying tropospheric ozone, OH, and NO_x concentrations (Figure 7) by conducting a sensitivity simulation where emissions of NMHCs (including ketones) were shut off. Without NMHCs, simulated ozone concentrations in the northern extratropics decrease by 10-20% in the lower troposphere and by a smaller amount in the upper troposphere. Similar decreases are found in the tropics. The decrease of ozone concentrations is less than 5% in the southern extratropics. The global annual mean burden of tropospheric ozone decreases by 8%.

Direct effect of NMHCs on ozone production is weak because this production is limited primarily by the supply of NO_x [*Chameides et al.*, 1992] including in the upper troposphere [*Jaegle et al.*, 1998]. More important is the indirect effect associated with perturbation of NO_x concentrations through formation of PAN (Figure 7b). This effect results in relatively large perturbations to ozone production rates at different altitudes in the troposphere, which, however, compensate for one another yielding little net perturbation to ozone concentrations. Figure 7a shows that suppressing NMHC emissions increases ozone production by up to 50% in the middle troposphere at 600-300 mbar, owing to an increase in NO_x concentrations; this effect is balanced by a 20-50% decrease of ozone production in the lower troposphere, where NO_x concentrations decrease in the absence of NMHC emissions. Ozone production above 300 mbar (particularly in the tropics) decreases in the simulation without NMHCs, despite an increase in NO_x concentrations, because of the importance of acetone photolysis as a source for HO_x radicals in the upper troposphere [*Singh et al.*, 1995; *Jaegle et al.*, 1997; *McKeen et al.*, 1997].

Without NMHCs in the model, we find that the global mean

Figures 7a, 7b

OH concentration in the model as measured by the lifetime of CH_3CCl_3 [*Prinn et al.*, 1995] increases by 20% (Figure 7b). This perturbation reflects the importance of NMHCs and their oxidation products as sinks for OH. The effect is most pronounced in the continental lower troposphere in summer, where NMHC emissions (including in particular isoprene emitted by vegetation) are abundant. At northern midlatitudes in winter, photochemistry in the continental lower troposphere is NMHC limited [*Jacob et al.*, 1995], and OH concentrations decrease when NMHC emissions are omitted. Decreases in OH are also found in the uppermost troposphere, where photolysis of acetone provides a major source for HO_x radicals.

Major changes in the distribution of NO_x are found in the simulation without NMHC chemistry (Figure 7b), reflecting the absence of PAN. In the polluted continental boundary layer, suppressing NMHC emissions causes NO_x concentrations to increase because the formation of PAN is a sink for NO_x. In the remote troposphere the absence of a NO_x source from PAN decomposition causes NO_x concentrations to decrease when NMHC emissions are omitted. Exceptions are the upper troposphere and the high northern latitudes in winter, where PAN decomposition is ineffective because of low temperatures; NO_x concentrations in these regions increase in the absence of NMHCs because shutting off PAN formation allows further long-range transport of NO_x from the polluted continents.

Omitting NMHC emissions in our simulation causes NO_x concentrations in the upper troposphere to increase by 20-100%, whereas *Moxim et al.* [1996] found a much smaller effect (<10%) in their global three-dimensional model study of NO_x-PAN chemistry. Differences in convective transport between the two models may be the cause of this discrepancy. The convection scheme in our model allows for direct transfer of NO_x from the boundary layer to the upper troposphere, enabling NO_x perturbations in the boundary layer to propagate to the upper troposphere more directly (see Figure 7b, July) than does the model of *Moxim et al.* [1996], where convection is treated as a diffusive process.

Our model results can also be compared with the previous analysis of NMHC effects on NO_x chemistry by *Kasting and Singh* [1986]. This analysis used a one-dimensional (vertical) model for marine and continental atmospheres at northern midlatitudes and included only light NMHCs ($\leq C_4$). In compared with *Kasting and Singh* [1986], we predict a greater sensitivity of NO_x to PAN formation in the continental lower troposphere because of our inclusion of isoprene chemistry. Biogenic emission of isoprene contributes significantly to PAN concentrations in our model, about 50% on average (Figure 8); isoprene alone accounts globally for half of the effects of all NMHCs on NO_x, OH, and ozone. In winter, we find a much smaller sensitivity of NO_x to PAN formation than do *Kasting and Singh* [1986] because we account for N_2O_5 hydrolysis in aerosols.

Figure 8

6. Conclusions

We have used a global three-dimensional model of tropospheric O_3-NO_x-hydrocarbon chemistry to investigate the origin of ozone in different regions of the troposphere. On a global scale, the budget of tropospheric ozone is largely defined by a balance between in situ chemical production and loss within the troposphere; transport from the stratosphere accounts for only 9% of the global source of ozone in the troposphere, and deposition accounts for only 18% of the global sink. This close balance between chemical production and loss of ozone in the tropospheric column is maintained at all latitudes (except high latitudes in winter). It implies in particular that ozone in the tropical troposphere, which plays a key role in the global oxidizing capacity of the atmosphere, is sustained largely by tropical sources of NO_x.

We investigated further the origin of tropospheric ozone by tracing the transport and eventual removal of ozone produced in the stratosphere and in different regions of the troposphere. Results show that ozone concentrations at all altitudes in the troposphere reflect significant contributions from sources in the upper, middle, and continental lower troposphere. Vertical transport allows these different sources to extend their influence over the depth of the tropospheric column. The slower production of ozone in the upper troposphere than in the lower troposphere is compensated for by the increase in the lifetime of ozone with altitude, allowing ozone produced in the upper troposphere to extend its range of influence over larger spatial scales. We find also that the middle troposphere is a major source region for ozone throughout the troposphere even though it is not a region of net ozone production.

Model results indicate that transport from the stratosphere contributes 20 to 60% of tropospheric ozone at midlatitudes in winter, 5 to 40% in summer, and 5 to 10% in the tropics, with larger proportions in the upper troposphere. Transport from the stratosphere makes a somewhat larger contribution to the global tropospheric ozone inventory (15%) than to the global tropospheric ozone source (9%) because it takes place in the extratropical upper troposphere, where the lifetime of ozone is longer than that in the middle and lower troposphere.

The model reproduces the springtime ozone maximum observed at remote sites in the northern extratropics. We find that this springtime maximum reflects a superimposition of seasonal maxima of ozone transported from the stratosphere (which peaks in late winter) and ozone produced in the troposphere (which peaks in late spring). Although ozone production in the troposphere peaks in summer, long-range transport of this ozone to remote regions is more efficient in spring when the lifetime of ozone is much longer than that in summer, resulting in a late spring peak. The particularly large springtime maximum observed at Mauna Loa Observatory (Hawaii) is explained in the model mostly by long-range transport of ozone pollution from Asia in spring. Our model results do not support previous hypotheses that wintertime accumulation of ozone or its precursors at northern high latitudes contributes significantly to the maximum.

Previous global models of tropospheric chemistry have often neglected NMHCs, which add considerable complexity to the chemical computation. We conducted a sensitivity simu-

lation with no emissions of NMHCs or ketones in the model. We find that the global mean OH concentration as measured by the lifetime of CH_3CCl_3 [*Prinn et al.*, 1995] increases by about 20% when emissions of NMHCs and acetone are omitted. The effect on ozone is relatively weak (5-20%), reflecting compensating influences from decreased ozone production below 600 mbar (20-50%), increased production at 300-600 mbar (0-50%), and decreased production above 300 mbar (0-20%). The large altitudinal variation in the NMHC effect on ozone production reflects the corresponding perturbations in NO_x concentrations, which are driven primarily by the important role of PAN as a reservoir for the long-range transport of NO_x. Without NMHCs and hence without PAN formation, NO_x concentrations in continental source regions increase by 50-150%, and concentrations above 400 mbar also increase by 20-100% owing to the transport from these source regions by deep convection. In contrast, concentrations of NO_x in the remote lower troposphere, which are maintained in part by decomposition of PAN, decrease by 20-50%. Biogenic emission of isoprene in the model accounts for about half of PAN formation and half of the effects of all NMHCs on NO_x, OH, and ozone, underscoring the need for improved understanding of the emissions and chemistry of isoprene.

References

Balkanski, Y. J., D. J. Jacob, R. Arimoto, and M. A. Kritz, Long-range transport of radon-222 over the North Pacific Ocean: Implications for continental influence, *J. Atmos. Chem., 14,* 353-374, 1992.

Bradshaw, J., S. B. Smyth, S. C. Liu, R. Newell, D. D. Davis, and S. T. Sandholm, Observed distributions of nitrogen oxides in the remote free troposphere from NASA Global Tropospheric Experiments, in press, *Rev. Geophys.*, 1998.

Carroll, M. A., and A. M. Thompson, NO_x in the non-urban troposphere, in *Progress and Problems in Atmospheric Chemistry*, edited by J. R. Barker, World Sci. Pub., River Ridge, N. J., 1995.

Chameides, W. L., and J. C. G. Walker, A photochemical theory for tropospheric ozone, *J. Geophys. Res., 78,* 8751-8760, 1973.

Chameides, W. L., D. D. Davis, M. O. Rodgers, J. Bradshaw, S. Sandholm, G. Sachse, G. Hill, G. Gregory, and R. Rasmussen, Net ozone photochemical production over the eastern and central North Pacific as inferred from GTE/CITE, 1, observations during fall 1983, *J. Geophys. Res., 92,* 2131-2152, 1987.

Chameides, W. L., D. D. Davis, G. L. Gregory, G. Sachse, and A. L. Torres, Ozone precursors and ozone photochemistry over eastern North Pacific during the spring of 1984 based on the NASA GTE/CITE, 1, airborne observations, *J. Geophys. Res., 94,* 9799-9808, 1989.

Chameides, W. L., et al., Ozone precursor relationship in the ambient atmosphere, *J. Geophys. Res., 97,* 6037-6055, 1992.

Crutzen, P. J., A discussion of the chemistry of some minor constituents in the stratosphere and troposphere, *Pure Appl. Geophys., 106-108,* 1385-1399, 1973.

Crutzen, P. J., Global tropospheric chemistry, in *Low-Temperature Chemistry of the Atmosphere*, NATO ASI Ser., vol. 121, G.K. edited by Moortgat et al., pp. 465-498, Springer-Verlag, New York, 1994.

Crutzen, P. J., and P. H. Zimmermann, The changing photochemistry of the troposphere, *Tellus, 43AB,* 136-151, 1991.

Danielsen, E. F., Stratosphere-troposphere exchange based on radioactivity, ozone, and potential vorticity, *J. Atmos. Sci., 25,* 502-518, 1968.

Dentener, F. J., and P. J. Crutzen, Reaction of N_2O_5 on tropospheric aerosols: Impact on the global distributions of NO_x, O_3, and OH, *J. Geophys. Res., 98,* 7149-7163, 1993.

Dibb, J. E., R. W. Talbot, and G. L. Gregory, Beryllium 7 and lead 210 in the western hemisphere arctic atmosphere: Observations from three recent aircraft-based sampling programs, *J. Geophys. Res., 97,* 16,709-16,715, 1992.

Dibb, J. E., D. Meeker, R. C. Finkel, J. R. Southon, M. W. Caffee, and L. A. Barrie, Estimation of stratospheric input to the Arctic troposphere: [7]Be and [10]Be in aerosols at Alert, Canada, *J. Geophys. Res., 99,* 12,855-12,864, 1994.

Dibb, J. E., R. W. Talbot, K. I. Klemm, G. L. Gregory, H. B. Singh, J. D. Bradshaw, and S. T. Sandholm, Asian influence over the western North Pacific during the fall season: Inferences from lead 210 and soluble ionic species and ozone, *J. Geophys. Res., 101,* 1779-1792, 1996.

Fan, S.-M., D. J. Jacob, D. L. Mauzerall, J. D. Bradshaw, S. T. Sandholm, D. R. Blake, H. B. Singh, R. W. Talbot, G. L. Gregory, and G. W. Sachse, Photochemistry of reactive nitrogen in the subarctic troposphere in summer 1990: Observation and modeling, *J. Geophys. Res., 99,* 16,867-16,878, 1994.

Fishman, J., Ozone in the troposphere, in *Ozone in the Free Atmosphere*, edited by R. C. Whitten and S. S. Prasad, pp. 161-194, Van Nostrand Reinhold, New York, 1985.

Follows, M. J., and J. F. Austin, A zonal average model of the stratospheric contributions to the tropospheric ozone budget, *J. Geophys. Res., 97,* 18,047-18,060, 1992.

Hansen, J., G. Russel, D. Rind, P. Stone, A. Lacis, S. Lebedeff, R. Ruedy, and L. Travis, Efficient three-dimensional global models for climate studies: Models I and II, *Mon. Weather Rev., 111,* 609-662, 1983.

Hirsch, A. I., J. W. Munger, D. J. Jacob, L. W. Horowitz, and A. H. Goldstein, Seasonal variation of the ozone production efficiency

per unit NO$_x$ at Harvard Forest, Massachusetts, *J. Geophys. Res., 101,* 12,659-12,666, 1996.

Honrath, R. E., and D. A. Jaffe, The seasonal cycle of nitrogen oxides in the Arctic troposphere at Barrow, Alaska, *J. Geophys. Res., 97,* 20,615-20,630, 1992.

Honrath, R. E., A. J. Hamlin, and J. T. Merrill, Transport of ozone precursors from the Arctic troposphere to the North Atlantic region, *J. Geophys. Res., 101,* 29,335-29,351, 1996.

Jacob, D. J., et al., Summertime photochemistry of the troposphere at high northern latitudes, *J. Geophys. Res., 97,* 16,421-16,431, 1992.

Jacob, D. J., J. A. Logan, G. M. Gardner, R. M. Yevich, C. M. Spivakovsky, S. C. Wofsy, S. Sillman, and M. J. Prather, Factors regulating ozone over the United States and its export to the global atmosphere, *J. Geophys. Res., 98,* 14,817-14,826, 1993.

Jacob, D. J., L. W. Horowitz, J. W. Munger, B. G. Heikes, R. R. Dickerson, R. S. Artz, and W. C. Keene, Seasonal transition from NO$_x$- to hydrocarbon-limited conditions for ozone production over the eastern United States in September, *J. Geophys. Res., 100,* 9315-9324, 1995.

Jacob, D. J., et al., The origin of ozone and NO$_x$ in the tropical troposphere: A photochemical analysis of aircraft observations over the South Atlantic Basin, *J. Geophys. Res., 101,* 24,235-24,250, 1996.

Jaegle, L., et al., Observed OH and HO$_2$ in the upper troposphere suggest a major source from convective injection of peroxides, *Geophys. Res. Lett., 24*, 3181-3184, 1997.

Jaegle, L., D. J. Jacob, W. H. Brune, D. Tan, I. Faloona, A. J. Weinheimer, B. A. Ridley, T. L. Campos, and G. W. Sachse, Sources of HO$_x$ and production of ozone in the upper troposphere over the United States, in press, *Geophys. Res. Lett.,* 1998.

Junge, C. E., Global ozone budget and exchange between stratosphere and troposphere, *Tellus, 14,* 363-377, 1962.

Kasting, J. F., and H. B. Singh, Nonmethane hydrocarbons in the troposphere: Impact on the odd hydrogen and odd nitrogen chemistry, *J. Geophys. Res., 91,* 13,239-13,256,1986.

Levy, H., II, J. D. Mahlman, W. J. Moxim, and S. C. Liu, Tropospheric ozone: The role of transport, *J. Geophys. Res., 90,* 3753-3772, 1985.

Liang, J., L. W. Horowitz, D. J. Jacob, Y. Wang, A. M. Fiore, J. A. Logan, G. M. Gardner, and J. W. Munger, Seasonal variation of photochemistry over North America and its implications for the export of ozone and reactive nitrogen to the global atmosphere, *J. Geophys. Res.*, in press, 1998.

Lin, W., M. Trainer, and S. C. Liu, On the nonlinearity of the tropospheric ozone production, *J. Geophys. Res., 93,* 7291-7297, 1988.

Liu, S. C., Model studies of background ozone formation, in *Tropospheric Ozone: Regional and Global Scale Interactions,* edited by I. S. A. Isaksen, 427 pp., D. Reidel, Norwell, Mass., 1988.

Liu, S. C., D. Kley, M. McFarland, J. D. Mahlman, and H. Levy II., On the origin of tropospheric ozone, *J. Geophys. Res., 85,* 7546-7552, 1980.

Liu, S. C., M. Trainer, F. C. Fehsenfeld, D. D. Parrish, E. J. Williams, D. W. Fahey, G. Hubler, and P. C. Murphy, Ozone production in the rural troposphere and the implications for regional and global ozone distributions, *J. Geophys. Res., 92,* 10,463-10,482, 1987.

Liu, S. C., et al., A study of the photochemistry and ozone budget during the Mauna Loa Observatory Photochemistry Experiment, *J. Geophys. Res., 97,* 10,463-10,471, 1992.

Logan, J. A., Tropospheric ozone: Seasonal behavior, trends, and anthropogenic influence, *J. Geophys. Res., 90,* 10,463-10,482, *J. Geophys. Res.*, 1985.

Logan, J. A., Ozone in rural areas of the United States, *J. Geophys. Res., 94,* 8511-8532, 1989.

McKeen, S. A., T. Gierczak, J. B. Burkholder, P. O. Wennberg, T. F. Hanisco, E. R. Keim, A. R.-S. Gao, S. C. Liu, A. R. Ravishankara, and D. W. Fahey, The photochemistry of acetone in the upper troposphere: A source of odd-hydrogen radicals, *Geophys. Res. Lett., 24,* 3177-3180, 1997.

Merrill, J. T., Atmospheric long range transport to the Pacific Ocean, in *Chemical Oceanography*, 10, edited by J. P. Riley and R. Duce, pp. 15-50, Academic, San Diego, Calif., 1989.

Moxim, W. J., H. Levy II, and P. S. Kasibhatla, Simulated global tro-

pospheric PAN: Its transport and impact on NO_x, *J. Geophys. Res., 101,* 12,621-12,638, 1996.

Müller, J.-F., and G. Brasseur, IMAGES: A three-dimensional chemical transport model of the global troposphere, *J. Geophys. Res., 100,* 16,445-16,490, 1995.

Penkett, S. A., and K. A. Brice, The spring maximum in photo-oxidants in the northern hemisphere troposphere, *Nature, 319,* 655-657, 1986.

Prinn, R. G., R. F. Weiss, B. R. Miller, J. Huang, F. N. Alyea, D. M. Cunnold, P. J. Fraser, D. E. Hartley, and P. G. Simmonds, Atmospheric trends and lifetime of CH_3CCl_3 and global OH concentrations, *Science, 269,* 187-192, 1995.

Prospero, J. M., R. Schmitt, E. Cuevas, D. L. Savoie, W. C. Graustein, K. K. Turekian, A. Volz-Thomas, A. Diaz, S. J. Oltmans, and H. Levy II., Temporal variability of summer-time ozone and aerosols in the free troposphere over the eastern North Atlantic, *Geophys. Res. Lett., 22,* 2925-2928, 1995.

Ridley, B. A., E. L. Atlas, J. G. Walega, G. L. Kok, T. A. Staffelbach, J. P. Greenberg, F. E. Grahek, P. G. Hess, and D. D. Montzka, Aircraft measurements made during the spring maximum of ozone over Hawaii: Peroxides, CO, O_3, NO_y, condensation nuclei, selected hydrocarbons, halocarbons, and alkyl nitrates between 0.5- and 9- km altitude, *J. Geophys. Res., 102*, 18,935-18,961, 1997.

Roelofs, G.-J., and J. Lelieveld, Distribution and budget of O_3 in the troposphere calculated with a chemistry general circulation model, *J. Geophys. Res., 100,* 20,983-20,998, 1995.

Roelofs, G.-J., and J. Lelieveld, Model study of the influence of cross-tropopause O_3 transport on tropospheric O_3 levels, *Tellus, 49B,* 38-55, 1997.

Sillman, S., J. A. Logan, and S. C. Wofsy, The sensitivity of ozone to nitrogen oxides and hydrocarbons in regional ozone episodes, *J. Geophys. Res., 95,* 1817-1851, 1990.

Singh, H. B., and P. L. Hanst, Peroxyacetyl nitrate (PAN) in the unpolluted atmosphere: An important reservoir for nitrogen oxides, *Geophys. Res. Lett., 8,* 941-944, 1981.

Singh, H. B., M. Kanakidou, P. J. Crutzen, and D. J. Jacob, High concentrations and photochemical fate of oxygenated hydrocarbons in the global troposphere, *Nature, 378,* 50-54, 1995.

Wang, Y., D. J. Jacob, and J. A. Logan, Global simulation of tropospheric O_3-NO_x-hydrocarbon chemistry, 1, Model formulation, this issue(a).

Wang, Y., J. A. Logan, and D. J. Jacob, Global simulation of tropospheric O_3-NO_x-hydrocarbon chemistry, 2, Model evaluation and global ozone budget, this issue(b).

D. J. Jacob and J. A. Logan, Department of Earth and Planetary Sciences and Division of Engineering and Applied Sciences, Harvard University, Cambridge, MA 02138. (e-mail: djj@io.harvard.edu; jal@io.harvard.edu)

Y. Wang, School of Earth and Atmospheric Sciences, Georgia Institute of Technology, Atlanta, GA 30332-0340. (e-mail: yhw@eas.gatech.edu)

[1]Now at School of Earth and Atmospheric Sciences, Georgia Institute of Technology, Atlanta, Georgia.

Figure Captions (Single Column)

Figure 1. Zonally averaged monthly mean concentrations of ozone, OH, NO_x, and PAN simulated by the model as a function of pressure and latitude for January and July.

Figure 2. Zonally averaged sources and sinks of ozone in the tropospheric column as a function of latitude in the model. Shown are monthly means of in situ chemical production and loss, transport from the stratosphere, and dry deposition for January, April, July, and October. The abscissa scale is linear in sine of latitude. Production and loss of ozone are referenced to the odd oxygen (O_x) family (see text for details).

Figure 3. Percentage contributions from each source region to the zonal mean ozone concentrations simulated in the model for January and July (Figure 1). The five source regions are the stratosphere, the upper troposphere (150 to 400 mbar), the middle troposphere (400 to 700 mbar), and the continental and marine lower troposphere (below 700 mbar).

Figure 4. Simulated zonal mean gross and net production rates of ozone (ppbv per day) and ozone lifetimes against chemical loss (days) as a function of pressure and latitude for January and July. Production and loss of ozone are referenced to the odd oxygen (O_x) family (see text for details).

Figure 5. Simulated and observed seasonal variations of ozone concentrations at Goose Bay, Canada (800 mbar) and at Mauna Loa Observatory, Hawaii (660 mbar). Values are monthly mean deviations from the annual means. Observations (solid circles) are from the ozonesonde climatology of J. A. Logan (An analysis of ozonesonde data, 1, Its application in testing models of tropospheric chemistry, manuscript in preparation, 1998). The seasonal variations in the model (solid lines) are decomposed into contributions of ozone transported from the stratosphere (dashed lines) and ozone produced within the troposphere (dotted lines).

Figure 6. Simulated seasonal variation of zonal mean ozone concentrations in the lower troposphere at northern extratropical latitudes (30°-90°N, below 700 mbar). Values are monthly mean deviations from the annual means. The seasonal variations in the model (solid lines) are decomposed into contributions of ozone transported from the stratosphere (dashed lines) and ozone produced within the troposphere (dotted lines). The contribution of ozone produced in the continental lower troposphere (below 700 mbar) is shown with dashed-dotted lines. Separate panels are shown for remote and polluted regions; the remote regions are defined as the ensemble of 4°x5° grid squares with NO_x emission from fossil fuel combustion less than $2x10^{11}$ molecules cm^{-2} s^{-1}.

Figure 7a. Percentage changes of zonal mean concentrations and gross production rates of ozone in a simulation without NMHC emissions relative to the standard simulation. Results are shown for January and July. Solid contours indicate positive changes, and dotted contours indicate negative changes.

Figure 7b. Same as Figure 7a but for zonal mean OH and NO_x concentrations.

Figure 8. Percentage decreases of zonal mean concentrations of PAN in a simulation without emissions of isoprene relative to the standard simulation for January and July.

Figure Captions (Double Column)

Figure 1. Zonally averaged monthly mean concentrations of ozone, OH, NO_x, and PAN simulated by the model as a function of pressure and latitude for January and July.

Figure 2. Zonally averaged sources and sinks of ozone in the tropospheric column as a function of latitude in the model. Shown are monthly means of in situ chemical production and loss, transport from the stratosphere, and dry deposition for January, April, July, and October. The abscissa scale is linear in sine of latitude. Production and loss of ozone are referenced to the odd oxygen (O_x) family (see text for details).

Figure 3. Percentage contributions from each source region to the zonal mean ozone concentrations simulated in the model for January and July (Figure 1). The five source regions are the stratosphere, the upper troposphere (150 to 400 mbar), the middle troposphere (400 to 700 mbar), and the continental and marine lower troposphere (below 700 mbar).

Figure 4. Simulated zonal mean gross and net production rates of ozone (ppbv per day) and ozone lifetimes against chemical loss (days) as a function of pressure and latitude for January and July. Production and loss of ozone are referenced to the odd oxygen (O_x) family (see text for details).

Figure 5. Simulated and observed seasonal variations of ozone concentrations at Goose Bay, Canada (800 mbar) and at Mauna Loa Observatory, Hawaii (660 mbar). Values are monthly mean deviations from the annual means. Observations (solid circles) are from the ozonesonde climatology of J. A. Logan (An analysis of ozonesonde data, 1, Its application in testing models of tropospheric chemistry, manuscript in preparation, 1998). The seasonal variations in the model (solid lines) are decomposed into contributions of ozone transported from the stratosphere (dashed lines) and ozone produced within the troposphere (dotted lines).

Figure 6. Simulated seasonal variation of zonal mean ozone concentrations in the lower troposphere at northern extratropical latitudes (30°-90°N, below 700 mbar). Values are monthly mean deviations from the annual means. The seasonal variations in the model (solid lines) are decomposed into contributions of ozone transported from the stratosphere (dashed lines) and ozone produced within the troposphere (dotted lines). The contribution of ozone produced in the continental lower troposphere (below 700 mbar) is shown with dashed-dotted lines. Separate panels are shown for remote and polluted regions; the remote regions are defined as the ensemble of 4°x5° grid squares with NO_x emission from fossil fuel combustion less than $2x10^{11}$ molecules cm^{-2} s^{-1}.

Figure 7a. Percentage changes of zonal mean concentrations and gross production rates of ozone in a simulation without NMHC emissions relative to the standard simulation. Results are shown for January and July. Solid contours indicate positive changes, and dotted contours indicate negative changes.

Figure 7b. Same as Figure 7a but for zonal mean OH and NO_x concentrations.

Figure 8. Percentage decreases of zonal mean concentrations of PAN in a simulation without emissions of isoprene relative to the standard simulation for January and July.
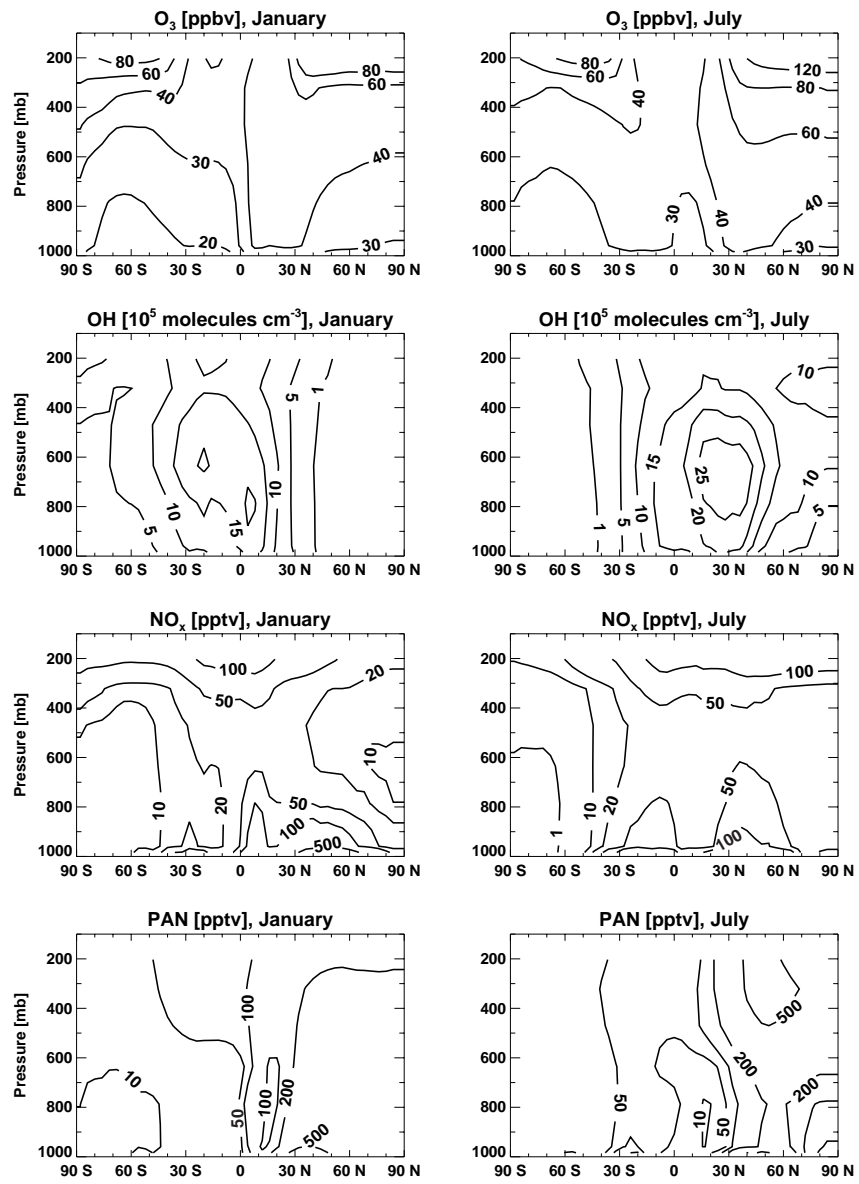
O₃ [ppbv], January
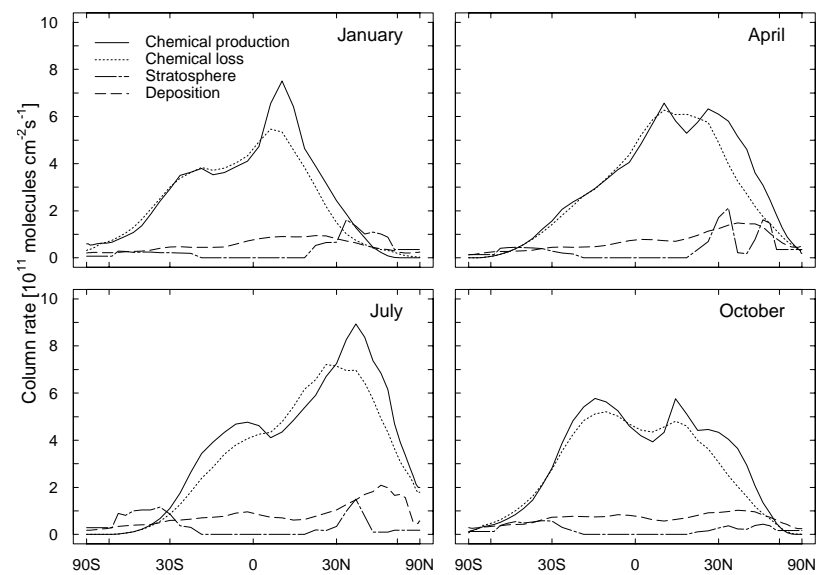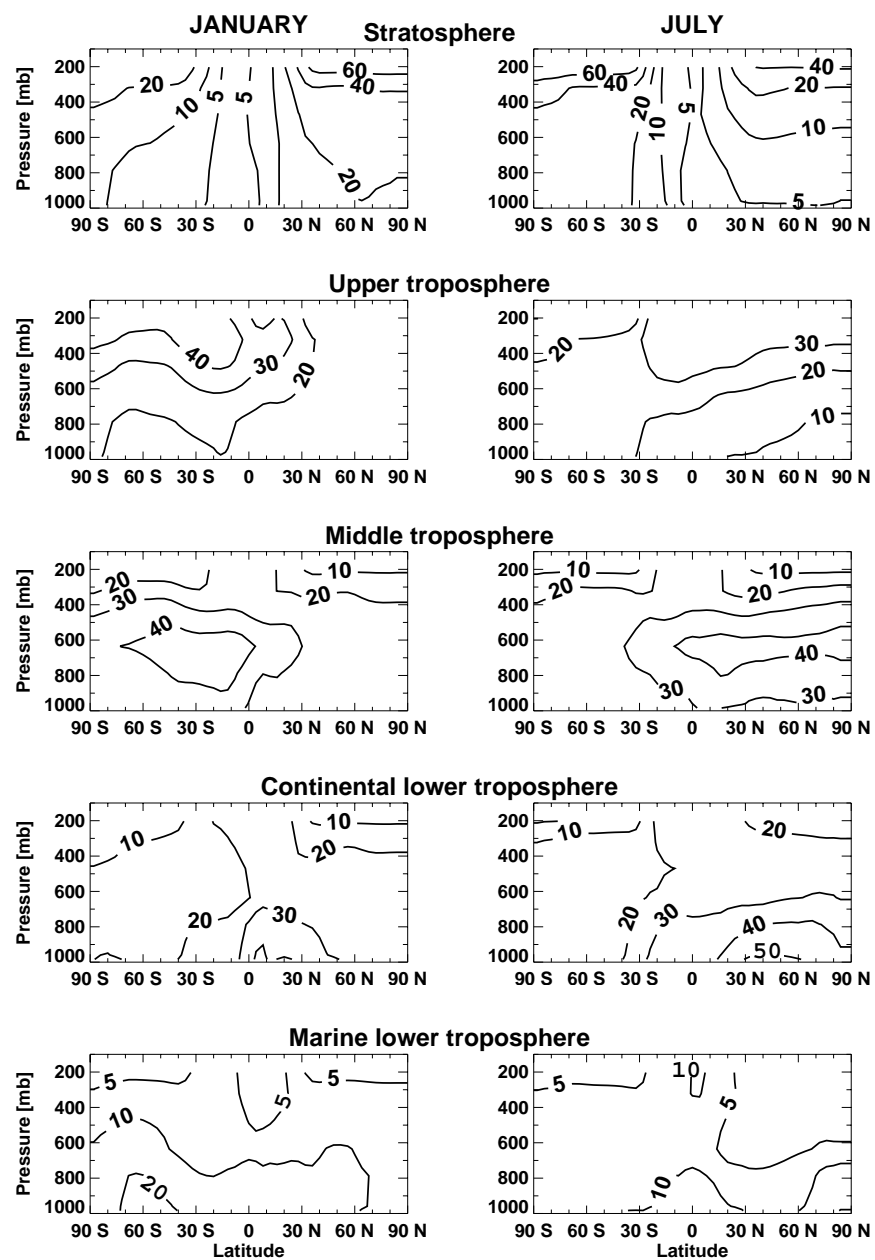
O₃ [ppbv], July

OH [10⁵ molecules cm⁻³], January

OH [10⁵ molecules cm⁻³], July

NOₓ [pptv], January

NOₓ [pptv], July

PAN [pptv], January

PAN [pptv], July

Fig. 1 (Bottom)

Fig. 2 (Bottom)

Fig. 3 (Bottom)

P(O₃) [ppbv day⁻¹], January
P(O₃) [ppbv day⁻¹], July
P-L (O₃) [ppbv day⁻¹], January
P-L (O₃) [ppbv day⁻¹], July
O₃ Chemical Lifetime [days], January
O₃ Chemical Lifetime [days], July
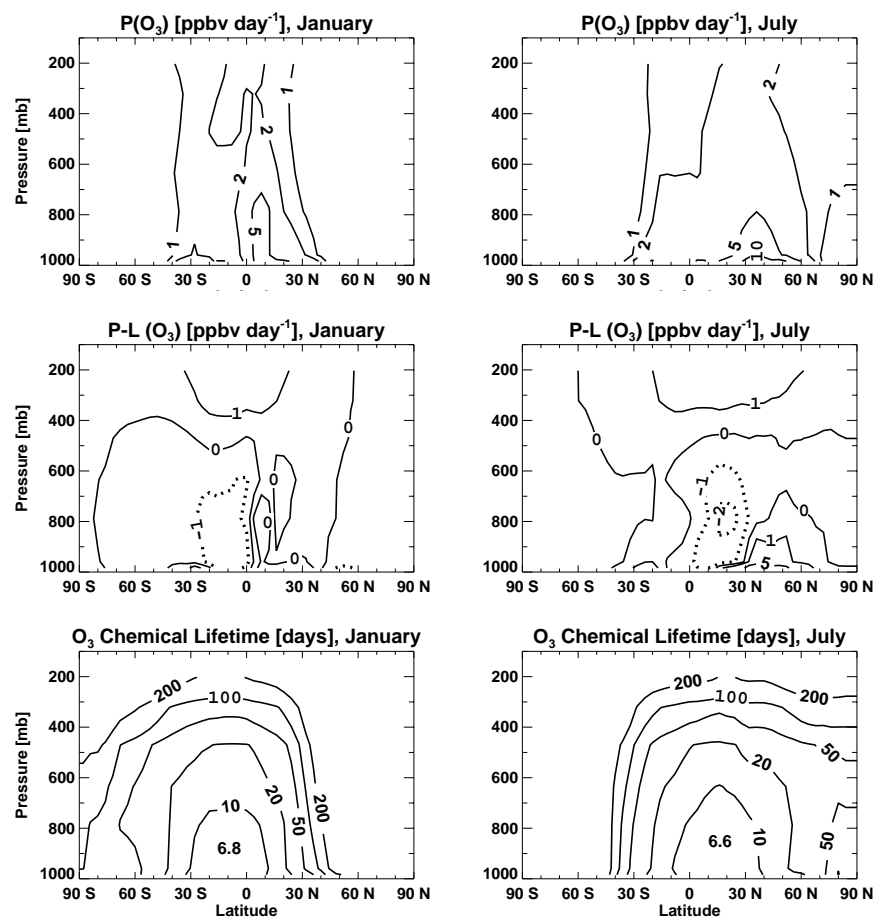
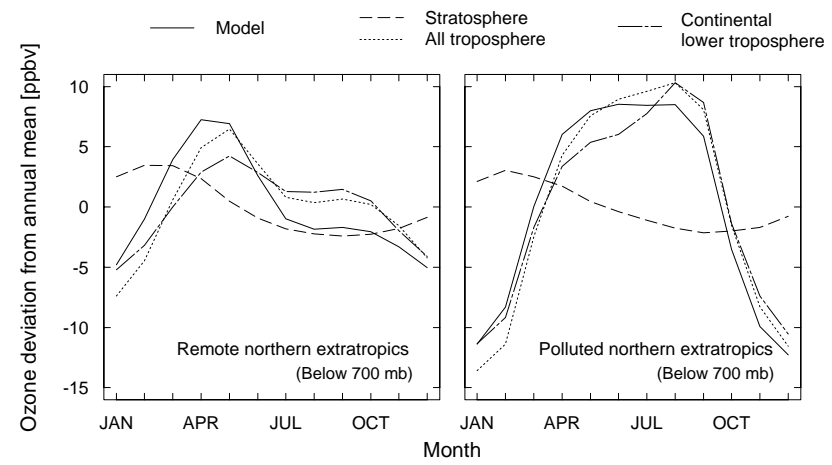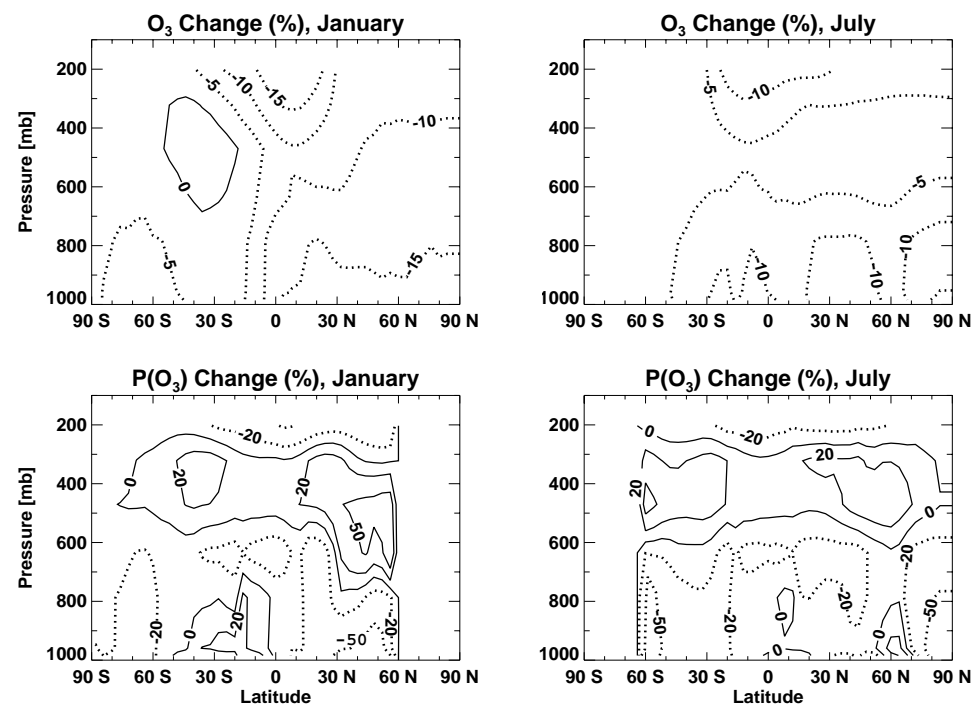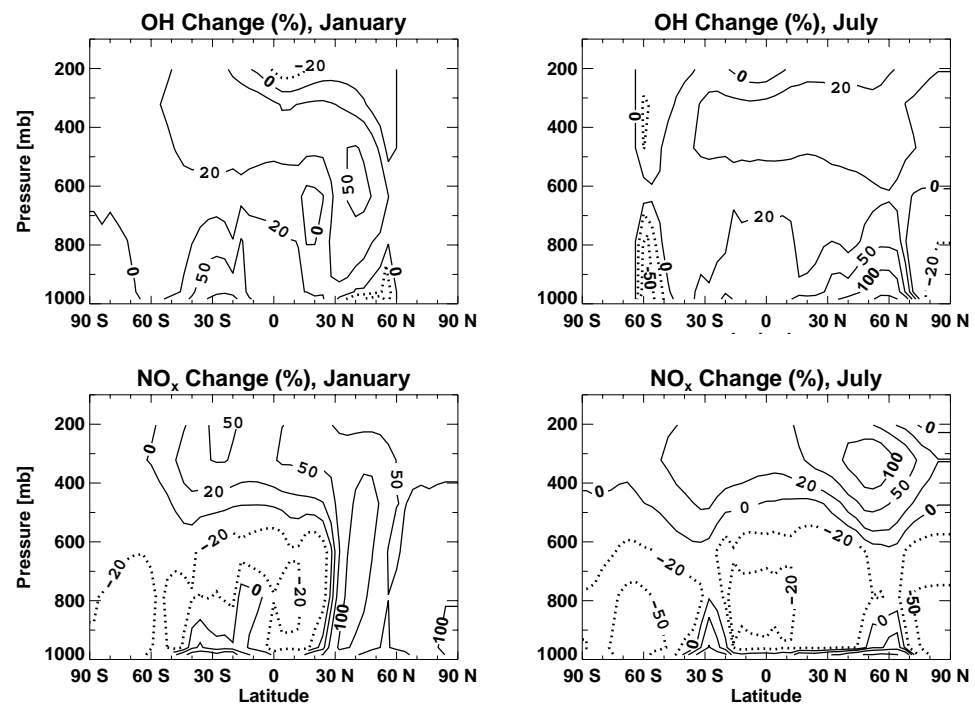Fig. 4 (Bottom)
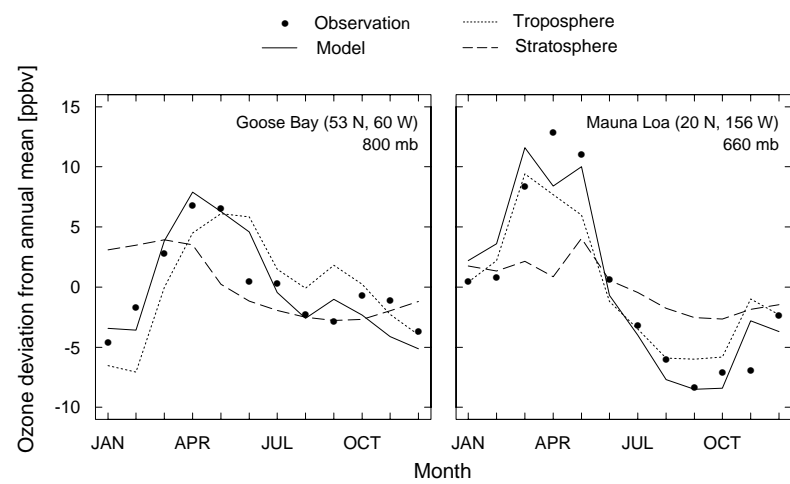
Fig. 5 (Bottom)

Fig. 6 (Bottom)

Fig. 7a (Bottom)

OH Change (%), January

OH Change (%), July

NO$_x$ Change (%), January

NO$_x$ Change (%), July

Fig. 7b (Bottom)

PAN Change (%), January   **PAN Change (%), July**

Fig. 8 (Bottom)